NANO EXPRESS   **Open Access**

The Potential Application of BAs for a Gas Sensor for Detecting SO$_2$ Gas Molecule: a DFT Study

Jian Ren[1*], Weijia Kong[2] and Jiaming Ni[3]

Abstract

Different atmospheric gas molecules (e.g., N$_2$, O$_2$, CO$_2$, H$_2$O, CO, NO, NO$_2$, NH$_3$, and SO$_2$) are absorbed on the pristine hexagonal boron arsenide (BAs) through density functional theory calculations. For each gas molecules, various adsorption positions were considered. The most stable adsorption depended on position, adsorption energy, charge transfer, and work function. SO$_2$ gas molecules had the best adsorption energy, the shortest distance for BAs surface in the atmospheric gas molecule, and a certain amount of charge transfer. The calculation of work function was important for exploring the possibilities of adjusting the electronic and optical properties. Our results presented BAs materials can be the potential gas sensor of SO$_2$ with high sensitivity and selectivity.

Keywords: Electronic structure, Density functional theory, Adsorption energy, Gas molecule, BAs

Introduction

BAs (hexagonal boron arsenide) is composed of groups III and V elements. The groups of III–V elements have excellent properties, such as excellent photoelectric properties, mechanical properties, and large band gap [1]. The promising potential applications of 2D materials [2–5] were well documented in recent studies [6–20]; these materials had been used to recognize various biomolecules [21, 22], pollutants [23, 24], and gas molecules [25, 26] to develop suitable sensing devices. We had found more and more the groups of III–V element materials, for example, BN, AlN, GaN, GaAs, and BP, and it has more and more studies for the gas molecules by theoretical calculation. Strak et al. [27] discovered AlN(0001) was a powerful catalyst for high-pressure-high-temperature synthesis of ammonia, and the work also confirmed the possibility of the efficient synthesis of ammonia at the AlN(0001) surface. Diao et al. [28] presented adsorption of H$_2$O, CO$_2$, CO, H$_2$, and N$_2$ on (10–10) surfaces of pristine and Zn-doped GaAs nanowires; the effect of the adsorption of CO$_2$ and N$_2$ on

absorption coefficients was the largest. Cheng et al. [29] showed the adsorption of most gas molecules on pure BP and doped BP by first principle study and concluded that N-BP was more suitable as a gas sensor for SO$_2$, NO, and NO$_2$ due to the existence of the desorption process. Kamaraj and Venkatesan [30] studied the structure and electronic properties of the BAs by the DFT and LDA; although considerable progress had been made in the experimental synthesis and theoretical study of BAs, the results of BAs nanosheets endowed the system with promising applications in nanoelectronics and photovoltaics.

In this work, we firstly investigated the gas sensing properties to fully exploit the possibilities of BAs as gas sensors by density functional theory (DFT) calculations. We predicted the adsorption properties of atmospheric gases (e.g., CO$_2$, O$_2$, N$_2$, H$_2$O, NO, NO$_2$, NH$_3$, CO, and SO$_2$) on BAs based on first principle calculations. Our work demonstrated the apparent adsorption behavior, moderate charge transfers, and unique transmission characteristics of SO$_2$ adsorption on BAs. The results suggested that monolayer BAs possessed great potential for SO$_2$ sensing application.

* Correspondence: 916181396@qq.com
[1]School of Computer Science and Technology, Huaiyin Normal University, Chang Jiang West Road 111, Huaian 223300, Jiangsu, China
Full list of author information is available at the end of the article

Theory and Method of Simulations

The system was modeled as a 4×4 supercell of BAs and atmospheric gas molecules adsorbed onto it. In DMol^3 [31] calculation process, exchange-correlation factions were calculated within a general gradient approximate (GGA) with the Perdew-Burke-Ernzerhof (PBE) [32]. The Brillouin zone was sampled using a $5 \times 5 \times 1$ Monkhorst-Pack k-point grid and Methfessel-Paxton smearing of 0.01 Ry. All the atomic structures were relaxed until the total energy and the Hellmann-Feynman force converged to 1.0×10^{-5} eV and 0.06 eV/Å [33].

To evaluate the interaction between gas molecules and adsorption sheet surface, we calculated the adsorption energy (E_{ad}) of adsorbed systems, which was defined as:

$$E_{ad} = E_{BAs+gasmolecule} - \left(E_{BAs} + E_{gas\ molecule}\right)$$

where $E_{BAs + gas\ molecule}$ is the total energy of BAs-adsorbed system, E_{BAs} is the energy of BAs, and $E_{gas\ molecule}$ is the energy of a gas molecule. All energies were calculated for optimized atomic structures. The charge transfer was investigated by Mulliken's population analysis.

Result and Discussion

Three adsorption sites were considered for BAs in this work, namely top of a boron atom (B), the top of an arsenic atom (As), and the center of a hexagonal B-As (center), as indicated in Fig. 1a. We studied the presence of the atmosphere and found the best gas sensor.

First of all, the geometric structure of pristine BAs monolayer had been optimized, and as shown in Fig. 1b, BAs bond length was 1.967 Å. There was an indirect band gap of 1.381 eV to exhibit in the band structure of BAs sheet, which was smaller than that of the bulk structure. These values were in good agreement with the previously reported values (Fig. 2) [34, 35].

Meanwhile, we had analyzed the adsorption energy, the charge transfer, and the distance between the molecules and BAs surface. The final result was as shown in Table 1.

N_2 adsorption: Adsorption of N_2 gas molecule on BAs was studied for three configurations of N_2/BAs, viz. top side of the B atom, top side of As atom, and the center of a hexagonal ring above the BAs surface, and the nearest distance was 3.764 Å, 3.549 Å, and 3.65 Å and corresponding adsorption energy was – 0.24 eV, – 0.27 eV, and – 0.24 eV, respectively. The center had the best adsorption energy and the most stable structure. The adsorption energy of N_2BAs was – 0.24 eV, the charge transfer from BAs to N^2 gas molecule was 0.014e, and the distance of the N2-BAs was 3.65 Å. Fig. 3a showed that there were many lines under the Fermi energy level, and the corresponding density of states had several peaks under the Fermi energy level. As shown in the figure, the N_2 gas molecule had four peaks, which had a certain influence on BAs, mainly from – 5 to 0 eV, and had great contributions to the DOS. Overall, the effect of N_2 gas molecule adsorption on BAs was poor.

O_2 adsorption: O_2 gas molecule tended to adsorb on the central point. The adsorption energy of O_2/BAs was – 0.35 eV, and the distance of the O_2-BAs was 2.90 Å. The total band structure and DOS for O_2/BAs were plotted in Fig. 3. It was obvious that an extra line crossed the zero point and reduced the band gap; O_2 gas molecule had a peak at – 1 to 0 eV and had an effect on the density of states above the Fermi level. The population analysis for Mulliken charge transfer showed that – 0.172e was transferred from BAs surface to the O_2 gas molecule, suggesting that O_2 gas molecule acted as an acceptor. In general, the O_2 gas molecule adsorption on BAs was better than N_2.

CO_2 adsorption: CO_2 gas molecule tended to adsorb on the top of As atom. The adsorption energy of CO^2/BAs was – 0.28 eV, the charge transfer from BAs to CO^2
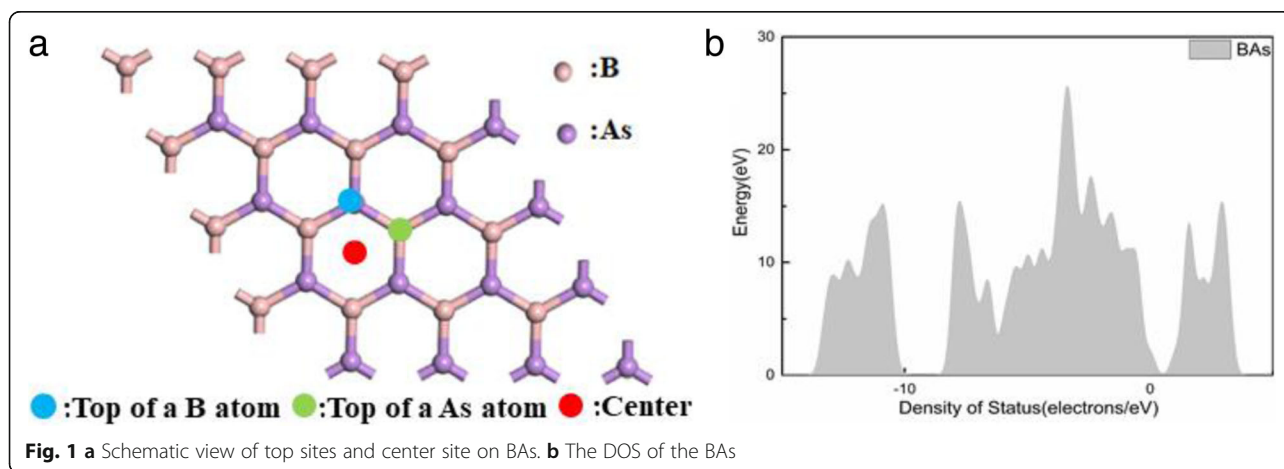

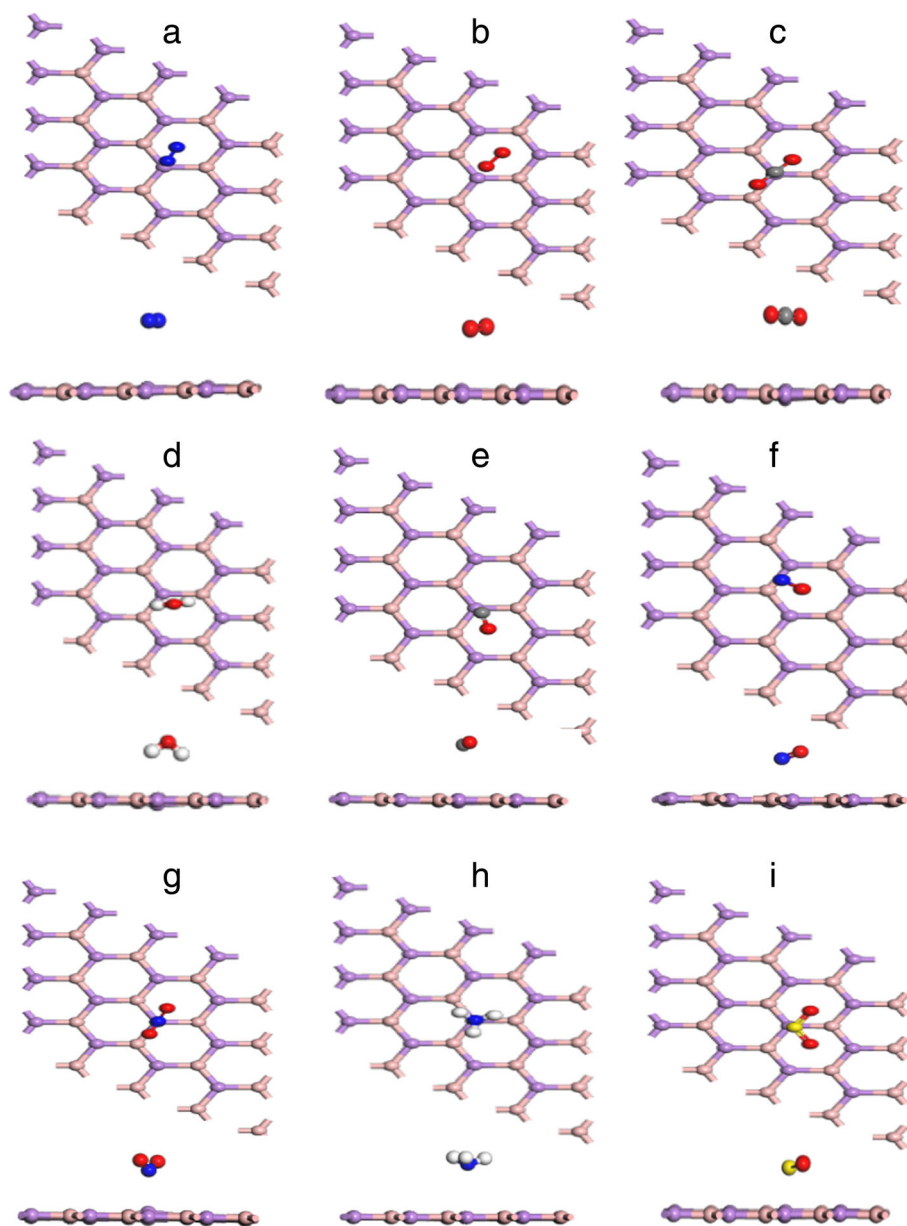**Fig. 1 a** Schematic view of top sites and center site on BAs. **b** The DOS of the BAs

Fig. 2 The most energetically favorable adsorption configurations of the gas molecules: N_2 (**a**), O_2 (**b**), CO_2 (**c**), H_2O (**d**), CO (**e**), NO (**f**), NO_2 (**g**), NH_3 (**h**), and SO_2 (**i**) on monolayer BAs

gas molecule was − 0.018e, and the distance of the CO^2-BAs was 3.55 Å. As shown in Fig. 3, compared to pristine BAs, the structure had no apparent change, and there were some obvious wave crests of the energy of − 9 eV in DOS, which had great contributions to the DOS. This point also highlighted the adsorption of CO_2 gas molecule by BAs. The results showed that the adsorption effect and sensitivity of BAs to CO_2 gas molecule were general.

H_2O adsorption: H_2O gas molecule tended to adsorb on the top of As atom. The adsorption energy of H^2O/BAs was − 0.38 eV, the charge transfer from BAs to H^2O

gas molecule was − 0.03e, and the distance of the H^2O-BAs was 3.63 Å. As shown in Fig. 3, there were no great changes in the structure compared to pristine BAs. The Fermi level of Al-G increased obviously and moved to the valence band. In general, the H_2O gas molecule adsorption on BAs was ignored.
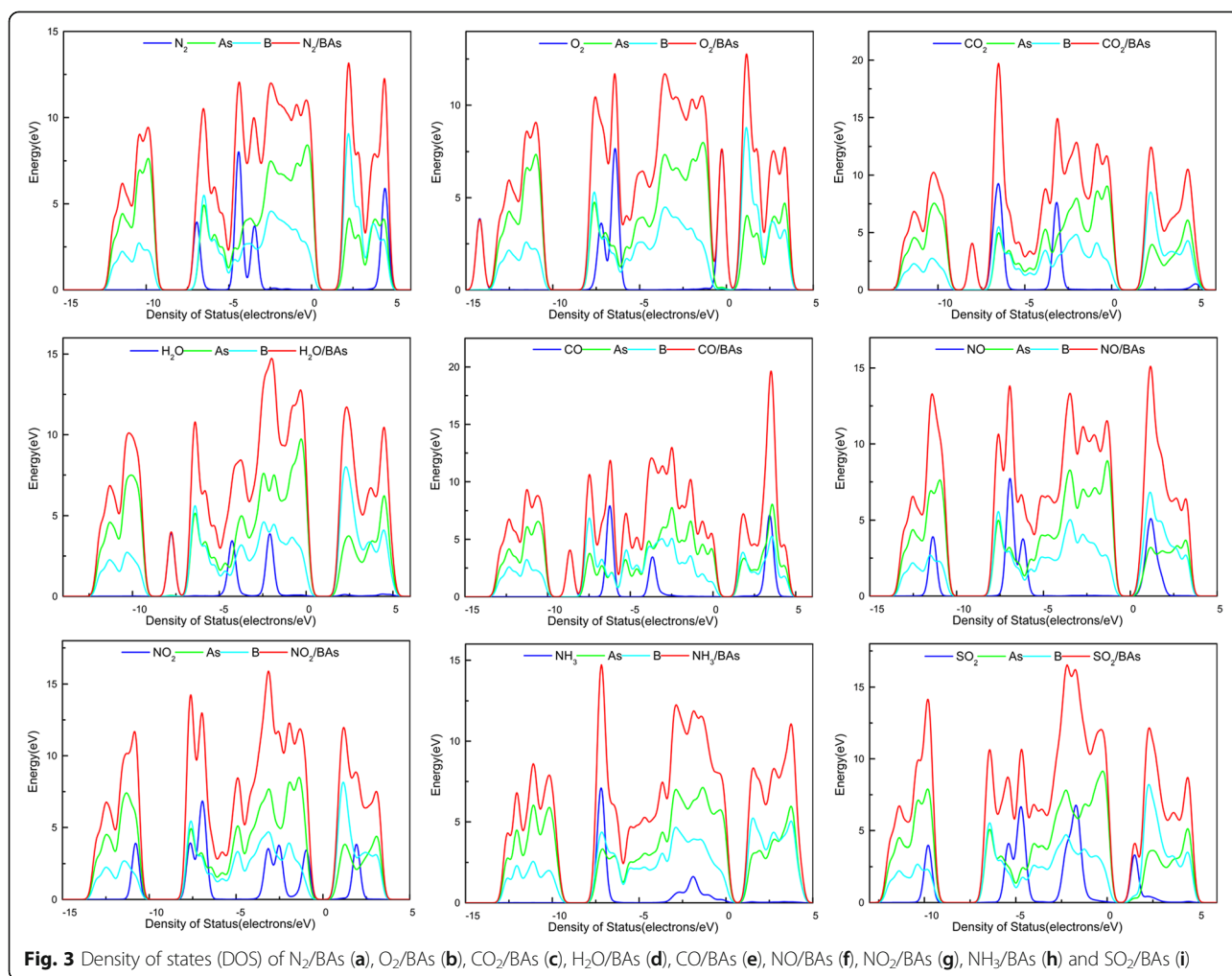
CO adsorption: CO gas molecule tended to adsorb on the top of As atom. The adsorption energy of CO/BAs was − 0.27 eV, the charge transfer from BAs to CO gas molecule was − 0.024e, and the distance of the CO-BAs was 3.50 Å. The total density of states (DOS) and band structure for BAs-CO were plotted in Fig. 3. CO gas

Table 1 Adsorption energy (E_{ad}), Mulliken charge (Q) from the molecule to monolayer BAs, and distance (gas molecule/BAs) of the equilibrium nearest atom of gas molecule to atom of BAs monolayer

System	E_{ad} (eV)	Q (e)	D (Å)	Style
N_2	− 0.24	− 0.014	3.65	Acceptor
O_2	− 0.35	− 0.172	2.90	Acceptor
CO_2	− 0.28	− 0.018	3.55	Acceptor
H_2O	− 0.38	− 0.030	3.63	Acceptor
CO	− 0.27	− 0.024	3.50	Acceptor
NO	− 0.18	0.010	2.86	Donor
NO_2	− 0.43	− 0.231	2.47	Acceptor
NH_3	− 0.34	0.007	3.27	Donor
SO_2	− 0.92	− 0.179	2.46	Acceptor

molecule and As atom played a huge role in the effect of a peak of 3 to 4 eV on the DOS. However, there was no deviation in DOS in − 7 to 4 eV range, which suggested that CO was weakly adsorbed on BAs. There was some obvious wave crest of the energy of − 3 to 1 eV and 3 eV, which had great contributions to the DOS. The population analysis for Mulliken charge transfer showed that − 0.024e charge was transferred from BAs surface to the CO gas molecule, and it suggested that CO gas molecule acted as an acceptor. Overall, the effect of CO gas molecule adsorption on BAs was not special.

NO adsorption: NO gas molecule tended to adsorb on the top of B atom. The adsorption energy of NO/BAs was − 0.18 eV, the charge transfer was − 0.01e from NO gas molecule to BAs, and the distance of the NO-BAs was 2.86 Å. There were a lot of lines upon the Fermi energy level. It found that the energy gap in the middle band reduced the band gap value. From the density diagram of states, there was an extra wave peak above the Fermi energy level, but there was little change under the Fermi energy level, relatively stable in Fig. 3. The mixing

Fig. 3 Density of states (DOS) of N_2/BAs (**a**), O_2/BAs (**b**), CO_2/BAs (**c**), H_2O/BAs (**d**), CO/BAs (**e**), NO/BAs (**f**), NO_2/BAs (**g**), NH_3/BAs (**h**) and SO_2/BAs (**i**)

of orbitals caused small charge transfer and redistribution over the interacting region. The population analysis for Mulliken charge transfer showed that 0.01e charge was transferred from BAs surface to the NO molecule, suggesting that NO acted as a donor. There was no deviation in DOS in − 7 to 4 eV range, which suggested that NO was weekly adsorbed on BAs.

NO$_2$ adsorption: NO$_2$ gas molecule tended to adsorb on the top of As atom. The adsorption energy of NO$_2$/BAs was − 0.43 eV, and the distance of the NO$_2$-BAs was 2.47 Å. The interesting was that the zero point in the band crossed a straight line directly after the adsorption of NO$_2$ gas molecule, which meant that the BAs, which is a semiconductor, was transformed into the gold attribute; band gap was 0 eV. There was no great change in the whole, and a peak was generated at about − 3 eV due to NO$_2$ gas molecular adsorption. There was some obvious wave crest of the energy of − 7 eV and 2 eV, which had great contributions to the DOS. In general, the adsorption of NO$_2$ by BAs was better than that of several molecules above.

NH$_3$ adsorption: NH$_3$ gas molecule tended to adsorb on the top of As atom. The adsorption energy of NH^3/BA was -0.34 eV, the charge transfer from NH^3 gas molecule to BA was 0.007e, and the distance of the NH^3-BA was 3.27 Å. There was no clear change in the energy band and the density of states, except that there was an obvious peak of adsorption of NH$_3$ gas molecule below the Fermi level. The NH$_3$ gas molecule had a little

impact on BAs at − 8 to − 4 eV, forming a 15 eV peak. The adsorption effect and sensitivity of its BAs to NH$_3$ gas molecule were general.

SO$_2$ adsorption: SO$_2$ gas molecule tended to adsorb on the central point, the adsorption energy of SO$_2$/BAs was − 0.92 eV, and the population analysis for Mulliken charge transfer showed that − 0.179e charge was transferred from BAs surface to the SO$_2$ gas molecule, suggesting that SO$_2$ gas molecule acts as an acceptor. The distance of the SO$_2$/BAs was 2.46 Å. Compared to other gas molecules, the SO$_2$/BAs had the biggest adsorption energy, the second largest electron transfer, and the shortest distance of the SO$_2$-BAs. As shown in Fig. 3, the valence band of BAs had an obvious up and band gap decreased, and due to the adsorbed SO$_2$ gas molecule, it could be seen from the density of states that there was one more wave peak at − 7.5 eV and certain transfer at the Fermi level. The adsorption of SO$_2$ by BAs had the excellent effect.

Fig. 4i showed the electron density diagram of SO$_2$/BAs and the electron local overlap between BAs and SO$_2$ gas molecule. On this basis, we drew the conclusion that the adsorption of SO$_2$ by BAs was physical adsorption. The calculation of WF shown in Fig. 5 was of great significance in exploring the possibility of regulating the electronic and optical properties (such as absorption spectra and energy loss functions) by adsorbing small molecules. The work function was defined in solid physics
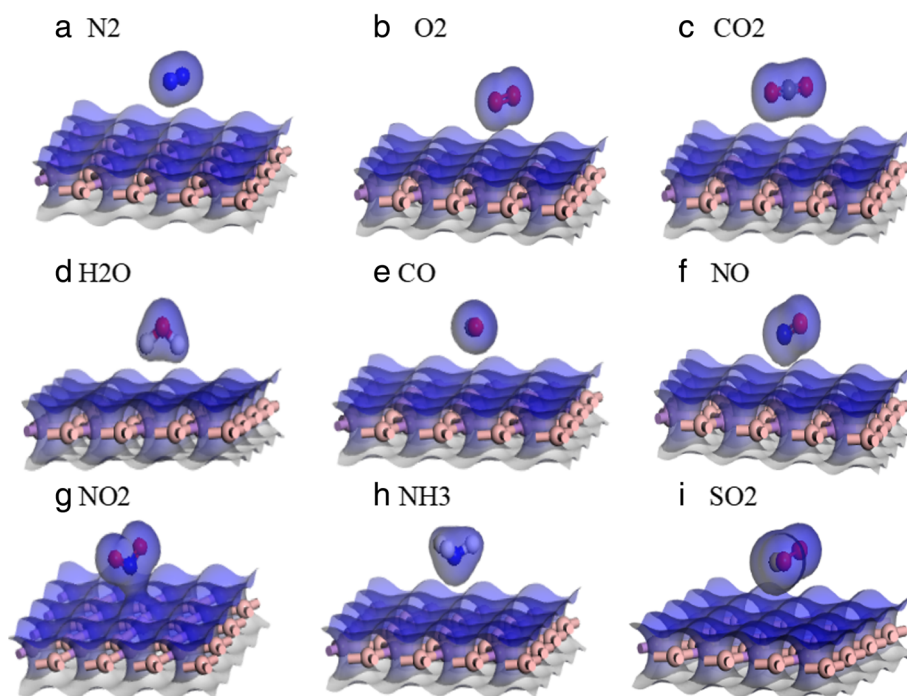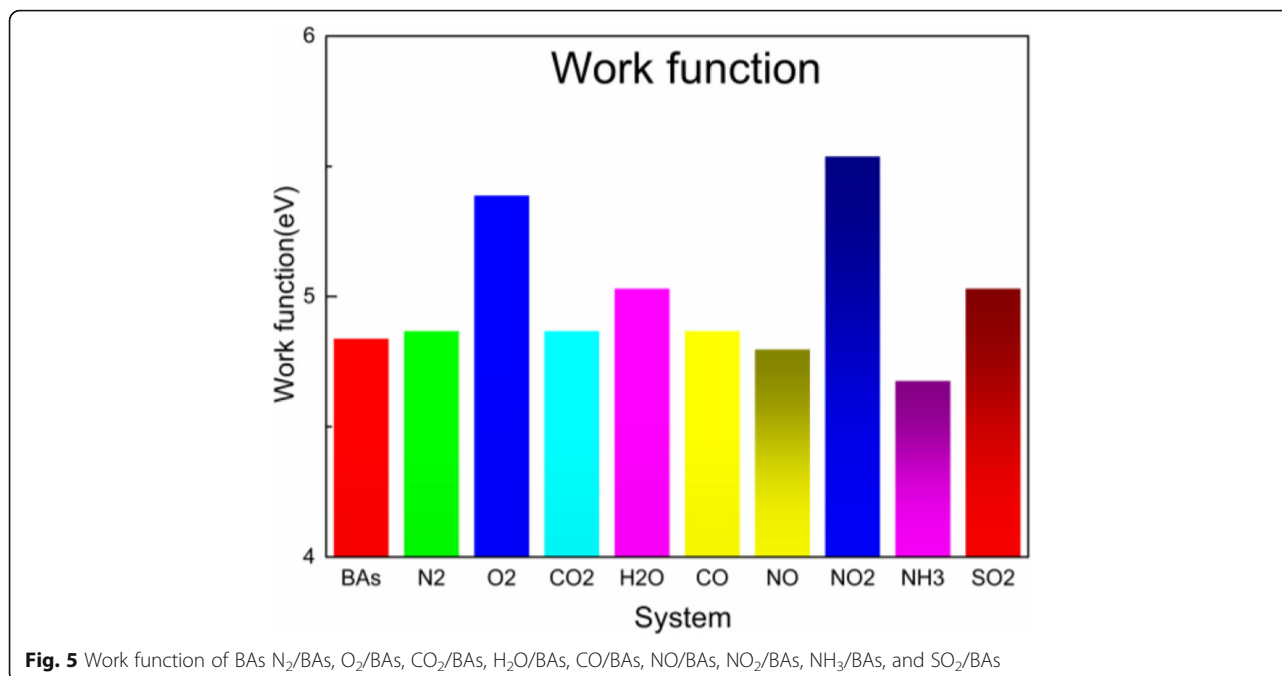

Fig. 4 Electron density for pristine N$_2$/BAs (**a**), O$_2$/BAs (**b**), CO$_2$/BAs (**c**), H$_2$O/BAs (**d**), CO/BAs (**e**), NO/BAs (**f**), NO$_2$/BAs (**g**), NH$_3$/BAs (**h**), and SO$_2$/BAs (**i**)

Fig. 5 Work function of BAs N_2/BAs, O_2/BAs, CO_2/BAs, H_2O/BAs, CO/BAs, NO/BAs, NO_2/BAs, NH_3/BAs, and SO_2/BAs

as the minimum energy required to move an electron from the interior of a solid to the surface of the object. The work function of pristine BAs was 4.84 eV. NO and NH_3 gas molecules were donors in charge transfer, and their work function decreased; the work function was 4.80 eV and 4.68 eV, respectively. The work function of N_2/BAs, CO_2/BAs, and CO/BAs was the same as that of BAs. The work function of O_2/BAs, NO_2/BAs, and SO_2/BAs was higher than BAs. Combined with the above adsorption energy, distance of gas molecules and BAs surface, charge transfer, and work function, we found that SO_2 gas molecule was most suitable for BAs materials.

Conclusion

We have presented the structural and electronic properties of BAs with adsorbents N_2, O_2, CO_2, H_2O, CO, NO, NO_2, NH_3, and SO_2 gas molecule, using density functional theory method. In the adsorption energy, $SO_2 > NO_2 > H_2O > O_2 > NH_3 > CO_2 > CO > N_2 > NO$ and $SO_2 < NO_2 < NO < O_2 < NH_3 < CO < CO_2 < H_2O < N_2$ in the adsorption distance. NO_2 has the largest Q and work function, maybe it could be detected by the proposed material because of good electrical response. SO_2 gas molecule had the best adsorption energy, the shortest distance for gas molecule and BAs surface, and a certain amount of charge transfer. Combined with the above adsorption energy, distance of gas molecule and BAs surface, charge transfer, and work function, the current and the adsorption-induced current change of BAs exhibit strong anisotropic characteristics. Such sensitivity and selectivity to SO_2

gas molecule adsorption make BAs a desirable candidate as a superior gas sensor.

Availability of Data and Materials
All data are fully available without restriction.

Authors' Contributions
JR and WK designed and carried out the experiments and drafted the manuscript. JMN participated in the work to analyze the data and gave the materials and supporting software. All authors read and approved the final manuscript.

Authors' Information
Not applicable

Competing Interests
The authors declare that they have no competing interests.

Publisher's Note
Springer Nature remains neutral with regard to jurisdictional claims in published maps and institutional affiliations.

Author details
[1]School of Computer Science and Technology, Huaiyin Normal University, Chang Jiang West Road 111, Huaian 223300, Jiangsu, China. [2]Department of Chemistry, Beijing Normal University, No.19, Waidajie, Xinjiekou, Haidian District, Beijing 100875, China. [3]School of Mechanical and Electrical Engineering, Guilin University of Electronic Technology, Jinji Road No.1, 54100 Gui, China.

References

1. Lindsay L, Broido DA, Reinecke TL (2013) First-principles determination of ultrahigh thermal conductivity of boron arsenide: a competitor for diamond. Phys Rev Lett 111(2):025901
2. Xu M, Liang T, Shi M et al (2013) Graphene-like two-dimensional materials. Chem Rev 113(5):3766–3798
3. Miró P, Audiffred M, Heine T (2014) An atlas of two-dimensional materials. Chem Soc Rev 43(18):6537
4. Zhang S, Yan Z, Li Y et al (2015) Atomically thin arsenene and antimonene: semimetal–semiconductor and indirect–direct band-gap transitions. Angewandte Chemie 127(10):3155–3158
5. Zhang S, Zhou W, Ma Y et al (2017) Antimonene oxides: emerging tunable direct bandgap semiconductor and novel topological insulator. Nano Lett 17(6):3434–3440
6. Perreault F, Fonseca d FA, Elimelech M (2015) Environmental applications of graphene-based nanomaterials. Chem Soc Rev 46(39):5861–5896
7. Zhang S, Guo S, Chen Z et al (2017) Recent progress in 2D group-VA semiconductors: from theory to experiment. Chem Soc Rev 468:209–222
8. Zhou W, Guo S, Zhang S et al (2018) DFT coupled with NEGF study of a promising two-dimensional channel material: black phosphorene-type GaTeCl. Nanoscale 10(7):3350–3355
9. Bhimanapati GR, Lin Z, Meunier V et al (2015) Recent advances in two-dimensional materials beyond graphene. Acs Nano 9(12):11509–11539
10. Lin Y, Connell JW (2012) Advances in 2D boron nitride nanostructures: nanosheets, nanoribbons, nanomeshes, and hybrids with graphene. Nanoscale 4(22):6908–6939
11. Hinnemann B, Moses PG, Bonde J et al (2005) Biomimetic hydrogen evolution: MoS2, nanoparticles as catalyst for hydrogen evolution. J Am Chem Soc 36(25):5308–5309
12. Umadevi D, Panigrahi S, Sastry GN (2014) Noncovalent interaction of carbon nanostructures. Acc Chem Res 47(8):2574–2581
13. Weng Q, Wang X, Wang X et al (2016) Functionalized hexagonal boron nitride nanomaterials: emerging properties and applications. Chem Soc Rev 45(14):3989–4012
14. Novoselov KS, V I F'K, Colombo L et al (2012) A roadmap for graphene. Nature 490(7419):192–200
15. Li J, Fan H, Jia X (2010) Multilayered ZnO nanosheets with 3D porous architectures: synthesis and gas sensing application. J Phys Chem C 114(35):14684–14691
16. Tian H, Fan H, Li M et al (2015) Zeolitic imidazolate framework coated ZnO nanorods as molecular sieving to improve selectivity of formaldehyde gas sensor. ACS Sensors 1(3):243–250
17. Ma L, Fan H, Tian H et al (2016) The n-ZnO/n-In2O3 heterojunction formed by a surface-modification and their potential barrier-control in methanal gas sensing. Sensors Actuators B Chem 222:508–516
18. Wang W, Fan H, Ye Y (2010) Effect of electric field on the structure and piezoelectric properties of poly (vinylidene fluoride) studied by density functional theory. Polymer 51(15):3575–3581
19. Liu K, Fan H, Ren P et al (2011) Structural, electronic and optical properties of BiFeO3 studied by first-principles. J Alloys Compounds 509(5):1901–1905
20. Liu X, Fan HQ (2018) Electronic structure, elasticity, Debye temperature and anisotropy of cubic WO3 from first-principles calculation. Royal Soc Open Sci 5(6):171921
21. He S, Song B, Li D et al (2010) A graphene nanoprobe for rapid, sensitive, and multicolor fluorescent DNA analysis. Adv Func Mat 20(3):453–459
22. Mudedla SK, Balamurugan K, Kamaraj M et al (2015) Interaction of nucleobases with silicon doped and defective silicon doped graphene and optical properties. Phys Chem Chem Phys 18(1):295–309
23. Setiadi A, Shafiul Alam M, Muttaqien F et al (2013) Hydrogen adsorption in capped armchair edge (5,5) carbon nanotubes. Jap J Appl Phys 52(12):599–602
24. Shautsova V, Gilbertson AM, Black NCG et al (2016) Hexagonal boron nitride assisted transfer and encapsulation of large area CVD graphene. Sci Rep 6:30210
25. Schedin F, Geim AK, Morozov SV et al (2006) Detection of individual gas molecules adsorbed on graphene. Nat Mat 6(9):652–655
26. Varghese SS, Lonkar S, Singh KK et al (2015) Recent advances in graphene based gas sensors. Sensors Actuators B Chem 218:160–183
27. Strak P, Sakowski K, Kempisty P et al (2018) Adsorption of N2 and H2 at AlN (0001) surface: ab initio assessment of the initial stage of ammonia catalytic synthesis. J Phys Chem C 122(35):20301–20311
28. Diao Y, Liu L, Xia S (2018) Adsorption of residual gas molecules on (10–10) surfaces of pristine and Zn-doped GaAs nanowires. J Mat Sci 53(20):14435–14446
29. Cheng Y, Meng R, Tan C et al (2018) Selective gas adsorption and I–V response of monolayer boron phosphide introduced by dopants: afirst-principle study. Appl Surf Sci 427:176–188
30. Manoharan K, Subramanian V (2018) Exploring multifunctional applications of hexagonal boron arsenide sheet: a DFT study. ACS Omega 3
31. O.-T W J (1984) Molecular mechanics: by U. Burkert and N. L. Allinger, American Chemical Society, Washington. J Mol Struc Theochem 109(3–4):401–401
32. Delley B (1990) An all-electron numerical method for solving the local density functional for polyatomic molecules. J Chem Phys 92(1):508–517
33. Becke AD (1993) A new mixing of Hartree–Fock and local density-functional theories. J Chem Phys 98(2):1372–1377
34. Tong CJ, Zhang H, Zhang YN et al (2014) New manifold two-dimensional single-layer structures of zinc-blende compounds. J Mat Chem A 2(42):17971–17978
35. Zhuang HL, Hennig RG (2012) Electronic structures of single-layer boron pnictides. Appl Phys Lett 101(15):153109